NUREG/CR-3427
Vol. 1

Long-Term Performance of Materials Used for High-Level Waste Packaging

Quarterly Report
April - June 1983

Compiled by D. Stahl, N. E. Miller

Battelle Columbus Laboratories

Prepared for
U.S. Nuclear Regulatory Commission

GPO Printed copy price: $4.25

NUREG/CR-3427
Vol. 1

Long-Term Performance of Materials Used for High-Level Waste Packaging

Quarterly Report
April - June 1983

Manuscript Completed: June 1983
Date Published: August 1983

Compiled by
D. Stahl, N. E. Miller

Battelle Columbus Laboratories
505 King Avenue
Columbus, OH 43201

Prepared for
Division of Health, Siting and Waste Management
Office of Nuclear Regulatory Research
U.S. Nuclear Regulatory Commission
Washington, D.C. 20555
NRC FIN B6764

CONTRIBUTORS:

J. A. Beavers
H. J. Cialone
J. C. Cunnane
P. I. Feder
J. H. Holbrook
R. A. Holman
H. H. Krause
A. J. Markworth
J. K. McCoy
K. H. Moore
S. L. Nicolosi
M. R. Pascucci
S. P. Pednekar
S. W. Rust
E. D. Spinosa

ABSTRACT

The Nuclear Regulatory Commission is responsible for the licensing of deep-mined geologic repositories for high-level radioactive waste disposal. The NRC's Office of Nuclear Regulatory Research is developing the technical capability to assess the Department of Energy's compliance with applicable regulations. As part of the NRC's effort, Battelle's Columbus Laboratories is investigating the long-term performance of materials used for high-level waste packages. The experimental program for investigating waste form degradation is in preparation, and the mathematical description of waste glass dissolution has been refined. Groundwater corrosion studies have been nearly completed for titanium and are under way for steel container materials. Internal glass-stainless steel corrosion tests have been initiated and pitting chemical interactions are being evaluated. A first-cut physical description of general corrosion of container materials in contact with groundwaters is near completion. An improved description of fluid flow through a nuclear waste package was developed, along with a comprehensive method for tracking release of specific radioisotopes. Efforts continue in water-chemistry studies, accelerated testing, and procedure development.

This report documents investigations performed during April-June, 1983.

TABLE OF CONTENTS

LIST OF FIGURES

LIST OF TABLES

PREVIOUS REPORTS IN SERIES

NUREG/CR-3405, Volume 1: "Long-Term Performance of Materials Used for High-Level Waste Packaging: Annual Report, March 1982-April 1983."

1. INTRODUCTION

Battelle's Columbus Laboratories is presently carrying out this waste package performance program for the U.S. Nuclear Regulatory Commission (NRC). The objective is the development of sufficient understanding of the phenomena and processes which can lead to waste package containment failure and subsequent release of radionuclides. The NRC is responsible for regulatory actions concerning the construction and operation of deep mined geologic repositories that will contain high-level waste. These latter activities, as defined under the Nuclear Waste Policy Act of 1982, are the responsibility of the Department of Energy (DOE), which must submit an application to license the facility. The NRC will assess whether there is reasonable assurance that DOE's license application would comply with NRC regulations and EPA standards. The waste packages must provide containment of the waste over long periods of time after emplacement and must contribute to the control of radionuclide release so that the annual release of any radionuclide from the repository will be a small fraction of the inventory present 1000 years following repository closure, as per 10CFR60. Since NRC's compliance assessment requires the technical capability to understand relevant phenomena and processes relating to the long-term performance of the waste package, the NRC's Office of Nuclear Regulatory Research (RES) has established this program to provide that part of the input to the assessment As an important aid to this understanding, Battelle is developing technology which will serve as a research tool to integrate separate effects and predict the long-term performance of waste package materials. This will also assist in identifying and evaluating research needs.

Within the context of this project, the waste package is the waste form and the enclosing sealed container. The packing (or backfill material) placed in the space between the waste package and the repository borehole is of concern in that it may affect the performance of the waste package, but the performance of the packing is not in the scope of this project. The waste forms of interest are limited to those that have most potential for use by the DOE, namely borosilicate glasses and spent fuel. The container consists of one or more successive metallic enclosures that act as a barrier to the ingress of groundwater to the waste and the egress of radionuclides from the waste to the repository. The container also provides features for handling and transporting the waste during the operational phase. During fabrication, a glass waste form may be cast in a metallic container, generally called a canister, which acts as a contamination barrier and a means for handling the waste form. Type 304L stainless steel is the most prominent canister material being considered by the DOE. Any enclosure placed around the canister is called an overpack and may consist of more than one material or component. At the outset of the project, a potential overpack consisted of a thick-walled steel vessel which provided structural support for an outer thin-walled corrosion-resistant shell of a titanium alloy. The use of the titanium shell has subsequently been in less favor by DOE than just a sealed thick-walled low-carbon steel overpack. It is the plan to focus the attention of this research on those materials favored by DOE.

A major goal of the project is to utilize available pertinent information and not to duplicate the work of others. Consequently, an important early activity on the program was a thorough review and assessment of the pertinent literature regarding material properties, degradation mechanisms, and models. The key experiments and mechanism development requirements were then established. Also, baseline or reference experiments were outlined to confirm literature results for use so that the available information can be utilized to its maximum possible extent. Existing data and information provided by DOE and other NRC contractors on the conditions expected in the candidate repositories are utilized since they are important inputs to experiment design and modeling.

The main experimental program is focused on areas of need where data are unavailable from other sources. The studies are directed at the two primary components of the waste package: the container and the waste form. The container performance considers degradation by general corrosion, pitting corrosion, crevice corrosion, stress-corrosion cracking, hydrogen embrittlement, and mechanical stress. The waste-form studies emphasize the release of radionuclides primarily by dissolution of the waste form as it is affected by radiation damage, thermal aging, and mechanical stress.

The analytical studies are also carried out in parallel efforts. The degradation phenomena for the container and waste form which are identified by the experimentalists are described individually as "separate-effects" mechanisms. Simple mechanisms, such as a linear corrosion rate, have been utilized initially. These will be replaced by more comprehensive phenomenological descriptions as the program develops. In addition, probabilistic and statistical approaches will be added to assess the level of uncertainty and reliability of the data base and predictions.

This report describes the project accomplishments during the period April-June 1983. The first year's efforts were detailed in the first annual report, for the period April 1982-March 1983 (NUREG/CR-3405, Volume I). The present report contains four major sections, the first three of which (following this general introduction) correspond to the three major tasks of the project: Waste Forms, Container Materials, and System Description. The fifth section describes more generic activities which support the major tasks. Also included within each section is a short statement of near-term activities. Further detail on the planned activities can be found on the Year Two Work Plan.

2. WASTE FORMS

The first quarter's efforts in the waste form task have been devoted to finalizing the work plan, assembling and calibrating of equipment for leaching/corrosion experiments, and assessing various experimental schemes for testing radiation effects. Also, several QA procedures were prepared and are in the process of final approval.

Preparation of an acceptable work plan has taken an especially long time because of changes in NRC's thrust for this program. A new plan was prepared after meeting with NRC personnel to clarify project goals. Briefly, the new plan is directed toward identifyig and quantifying problems expected to be encountered by the waste form throughout its life from processing through disposal. The experimentation will be directed toward assessing the ability of waste forms to comply with the release rate criteria of 10CFR60.

The major problems identified for glass waste forms are thermal aging (devitrification) induced by processing conditions, aging by radiation effects, and leach/corrosion at varying repository conditions for numerous waste glass compositions. Devitrification studies have been minimal this quarter. The leaching/corrosion and radiation damage efforts will be discussed in separate report sections. In view of the new project requirements, the development of the topological model should be delayed. However, some NRC personnel have suggested that we consider the effect of composition variations on leaching/corrosion. A less comprehensive approach is suggested based on frits 76-101 (PNL 76-68 commercial glass) and SRL-131 (defense glass) to determine whether the topological model can predict leach/corrosion properties. This data will provide a basis for assessing the usefulness of the topological model to the NRC program.

2.1 Leaching/Corrosion

The start of the initial leaching/corrosion experiments has been frustrating. Most of the quarter's efforts in this area have been expended to meet operational and safety requirements for autoclaves operating at elevated temperature and pressures. Seemingly small tasks (such as valve replacement) have each resulted in delays in the project. A series of such occurrences has delayed the start of experimentation by about 6 weeks because the initial experiments require simultaneous operation of all three devices, one oven and two autoclaves. A test run of the autoclaves revealed that one heated at twice the rate of the other. This problem must be resolved or the experimental plan will have to be revised.

Testing of the temperature stability of the oven was completed in this project quarter. It achieved its maximum expected operating temperature, for this experiment, of 150 C in 60 minutes. Temperature stability was determined with a calibrated type K thermocouple to be 150 $\pm$3 C, which represents a 2 percent temperature control band. Such a band is adequate. Also, the oven temperature profile was checked at 74 C with a

type K thermocouple. The first test revealed that the temperature differential between the center and corners of the oven was too large. Two pieces of ceramic tile were placed in the bottom of the oven to provide thermal mass. These tiles reduced the temperature differential to ±1 C.

A preliminary test run in distilled water at 90 C using PNL 76-68 glass was conducted in this quarter. The pH change, measured at 30 C in a constant temperature bath, was 2.27 ±2 percent. The mean final solution pH was 9.05, which is in accord with literature data at these conditions. These data are for only nine samples, but they do show that our procedures are capable of reproducing data from the literature.

To maintain an anoxic condition in leaching/corrosion experiments, an argon atmosphere will be used. For lower temperature experiments conducted in the oven, the Teflon containers and specimens will be assembled in a glove box with an argon atmosphere. A purging procedure that will produce an oxygen concentration of <50 ppm was developed during the quarter. This procedure will reduce the CO_2 content to approximately 80 ppb, so its transfer to the corroding solutions and the concomitant buffering action should be largely eliminated.

2.2 Radiation Effects

The development of an experimental plan for studying radiation effects still poses major problems. The cost of studying transmutation in model glass systems is excessive for consideration on this project. Also, the simultaneous action of β/γ events are a potential problem area for waste form "aging." All of these problems need to be studied by accelerated "aging" experimentation, but such experimentation is not possible because more intense radiation sources than high-level-waste glass are not available. We are investigating the possibility of acquiring small portions of waste that have been prepared under waste isolation programs of other governments. The French and Canadians may have some vitrified waste that is rather old. If such wastes are available, they may be used to evaluate the severity of the postulated α, β/γ, and transmutation problems.

The Materials Characterization Center is offering a PNL 76-68 composition glass manufactured with real waste from reprocessed fuel. This material offers very little chance for accelerated "aging" other than temperature acceleration. Therefore, only a minimal quantity will be used in this program.

2.3 Glass-Dissolution Correlation

The description of the glass dissolution process that was originally derived for this program was based upon the limiting case of thermodynamic equilibrium, for which dissolution at the glass-water interface occurs so rapidly that the water becomes saturated with dissolved glass species virtually upon contact with the glass surface. Moreover, dissolution was assumed to occur congruently, with the glass solubility

limited by that of silica. Since these assumptions remove all other sources of time dependence, the kinetics of glass dissolution is thus controlled by the rate of flow of groundwater past the glass.

During this reporting period, some introductory consideration was given to effects that finite rates of glass dissolution would have upon the original flow-rate-controlled correlation. The results are now described.

Suppose that a volume V of groundwater is in contact with surface area S of glass and that the volumetric flow rate of the groundwater is $\dot{v}$. Let C be the instantaneous concentration, within the groundwater, of the glass component that controls the dissolution rate and let C_o be the equilibrium concentration of that component. The concentration C is assumed to be spatially invariant within V. This is clearly a simplified treatment, in which possible reactions that the species controlling dissolution (silica, in this case) may undergo, are not considered; it is assumed simply to accumulate, in solution, until its saturation level (assumed to vary only with temperature) is reached.

It is assumed further that the rate at which the species is transferred across the glass-water interface is directly proportional to the difference between its equilibrium and instantaneous concentration in the groundwater. The net rate at which the total amount of the species within V varies with time t is equal to the rate at which new amounts are added by dissolution minus the rate at which already-dissolved species are transported away by flow, i.e.,

$$V \frac{dC}{dt} = KS(C_o - C) - C\dot{v} \tag{1}$$

where K is a temperature-dependent rate constant. Equation 1 can be expressed in the alternative form

$$\frac{dC}{dt} + \frac{\alpha KS}{V} C = \frac{KS}{V} C_o \tag{2}$$

where

$$\alpha \equiv 1 + \frac{\dot{v}}{KS} \ . \tag{3}$$

Equation 2 can easily be solved, subject to the initial condition $C(t = 0) = 0$, to yield

$$C = \frac{C_o}{\alpha}\left[1 - \exp\left(-\frac{\alpha KS}{V} t\right)\right] \tag{4}$$

Let R_d be the instantaneous rate at which the species is dissolved from the glass. Clearly,

$$R_d = KS\,(C_o - C) \quad . \tag{5}$$

Combining Equations 3 to 5,

$$R_d = \frac{KSC_o}{\alpha}\left[\frac{\dot{v}}{KS} + \exp\left(-\frac{\alpha KS}{V}\,t\right)\right]. \tag{6}$$

Under steady-state conditions (that is, when the exponential term in Equation 6 becomes negligible), one obtains

$$R_d = C_o\dot{v}/\alpha \quad . \tag{7}$$

Combining Equations 3 and 7,

$$\rho = \frac{\nu}{1 + \nu} \tag{8}$$

where ρ and ν are normalized, dimensionless expressions for the dissolution rate and the flow rate, respectively, and are given by

$$\rho \equiv \frac{R_d}{KSC_o} \tag{9}$$

$$\nu \equiv \frac{\dot{v}}{KS} \quad . \tag{10}$$

Clearly, for $\nu << 1$, glass dissolution is flow-rate-controlled, with $\rho \simeq \nu$, i.e., $R_d \simeq C_o\dot{v}$. Conversely, for $\nu >> 1$, dissolution is controlled by transport of the species across the glass-water interface, with $\rho \simeq 1$, i.e., $R_d \simeq KSC_o$.

Equation 8 is plotted on logarithmic axes in Figure 1. At the lower flow rates, the curve is seen to approach a straight line having unit slope, whereas at the higher flow rates, it approaches a straight line having zero slope. These represent the two limiting cases discussed above.

The rate of release of the glass species to the environment can also be readily calculated, being equal to $C\dot{v}$. Under steady-state conditions, this quantity is equal to the rate of dissolution, as can be seen from Equation 1.

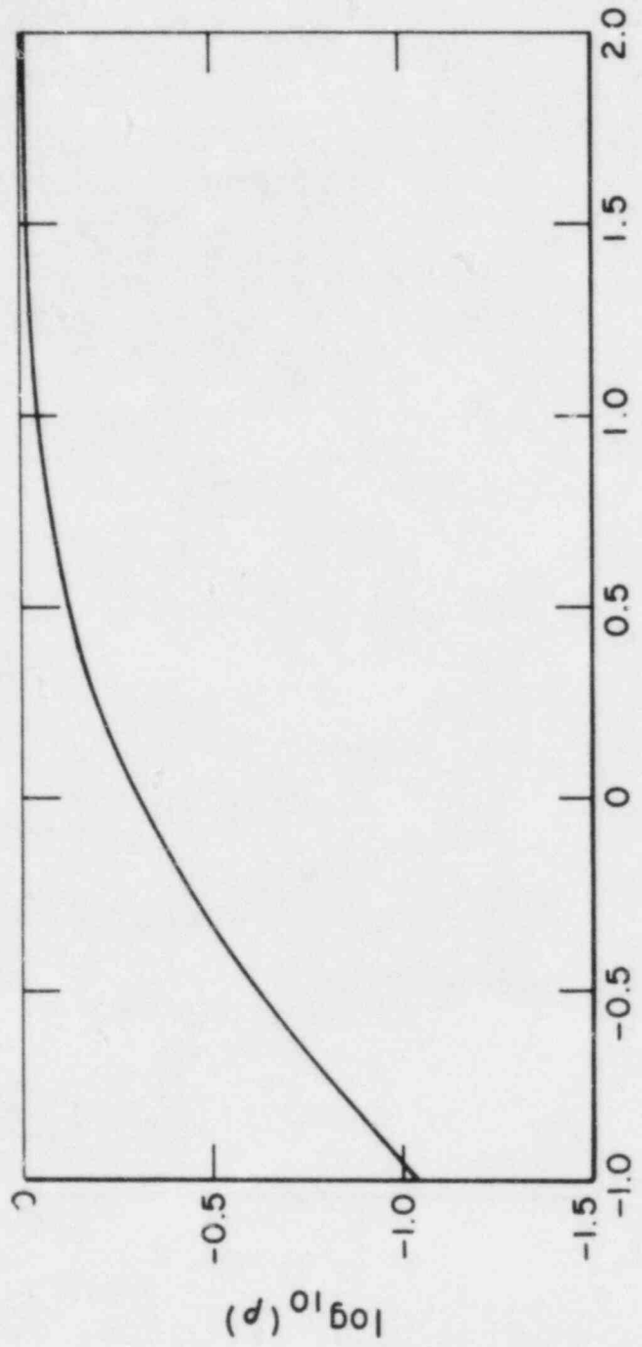

FIGURE 1. LOGARITHMIC PLOT OF ρ VERSUS ν (AFTER EQUATION 8)

3. CONTAINER MATERIALS

The container consists of two or more concentric metallic enclosures that act as a barrier against the ingress of groundwater (or brine) to the waste form and the egress of radionuclides from the waste form to the repository. The innermost metallic enclosure, called a canister, contains the waste form. For borosilicate glass, the most probable canister material is Type 304L stainless steel. The canister initially is subjected to internal corrosion as a result of contact with molten glass for short periods and hot glass for long periods. Later it could be subjected to groundwater attack if the outer enclosures fail. The outer enclosures are called the overpack. At the onset of the project, a potential overpack consisted of a thick-walled steel container and a thin-walled shell of titanium alloy. The use of a titanium shell has been subsequently in less favor by DOE so that the emphasis in this project was redirected appropriately.

3.1 Internal Corrosion

The experimental program was initiated during this quarter. It is designed to use a reference waste glass and modifications of the glass to determine the long-term corrosive effects on Type 304L stainless steel. The initial experiments are being conducted with a glass containing simulated waste and will investigate conditions expected to occur in the continuous-melting process.

3.1.1 Approach

Coupons of Type 304L stainless steel are being exposed to the waste glass in crucible tests under accelerated temperature conditions. Because the hydroxide (OH^-) content of the glass is expected to have an important influence on its corrosivity to stainless steel, the experiments will compare two levels of hydroxide content in the reference glass. The components in the glass that prove to be the most corrosive to the stainless steel will be identified. In subsequent experiments the concentration of these corrosive components will be varied within limits that might be expected to result from the high level wastes.

In order to predict long-term effects, the diffusion rates of the corrosive components to the glass-container interface must be known. If experimental data on the diffusion rates are lacking, the appropriate experiments will be performed to obtain the information needed. The information from the contact corrosion rate experiments and the diffusion rates will provide input for analyzing the long-term canister metal loss. Thus the prediction of the rate of internal attack will be based on the corrosion rates from the experimental data and the rates at which the corrosive agents will be supplied to the reaction zone at the canister wall by diffusion through the waste glass.

Materials

Ninety-six coupons of Type 304L stainless steel were prepared for the first set of experiments. The specimens are rectangular solids with the nominal dimensions 3.81 cm x 2.54 cm x 0.238 cm. The actual measured dimensions have the following ranges:

Length:	3.7732 - 3.8245 cm
Width:	2.5286 - 2.5585 cm
Thickness:	0.1925 - 0.2347 cm.

The specimen weight range is 14.5882 - 17.5339 g. Before measurement the specimens were polished to a 600 grit finish.

Crucibles of Type 304L stainless steel were fabricated by welding bases on short lengths of tubing. Forty-eight crucibles, with a diameter of 4 cm and a depth of 5 cm, were prepared. The certified analyses for the stainless steel sheet and tubing are shown in Table 1.

TABLE 1. CERTIFIED ANALYSES OF TYPE 304L STAINLESS STEEL

	Composition, weight percent	
	Sheet	Tubing
Carbon	0.017	0.016
Manganese	1.44	1.72
Phosphorus	0.026	0.024
Sulfur	0.010	0.013
Silicon	0.58	0.43
Chromium	18.29	18.64
Nickel	8.63	8.66
Molybdenum	0.29	--

A 12 kg supply of PNL 76-68 reference simulated waste glass has been obtained from the Pacific Northwest Laboratories. This glass is composed of two parts Frit 76-101 and one part Waste Type PW-8a. The chemical composition of the particular lot from which the supply was obtained is shown in Table 2.

Procedure

The metal coupons are being exposed to the 76-68 reference waste glass in muffle furnaces at temperatures of 900, 500, and 300 C. Approximately 120 g of the glass was melted in each crucible at 1000 C, and two metal specimens were then immersed in each crucible. There are 32 specimens being exposed at each of the three temperatures.

3.1.2 Results

After 400 hours' exposure, 6 coupons were removed from the 900 C furnace. These coupons were in three crucibles located at the rear, center, and front of the furnace. When the specimens were removed from the crucibles, the glass adhered to the surfaces in varying amounts for the different specimens. Most of this glass could be broken away, but enough remained so that weight change measurements would not be valid.

Micrometer measurements of specimen dimensions in areas where there was no residual glass showed increases up to 30 micrometers in thickness. This increase is indicative of either oxidation or reaction with the glass components. The nature of the reacted film on the surface will be determined by X-ray dispersive analysis in the scanning electron microscope.

Each specimen was sectioned across the width at the center line and one of the cut surfaces was mounted and polished. The edges which had been in contact with the glass were then examined for pitting attack, using the optical microscope. Most of the specimens showed a large number of small pits, about 20 micrometers deep, as shown in Table 3. The pit depths ranged from 20 to 120 micrometers, but relatively few of the deeper pits were observed. There appears to be some effect of position in the furnace, as specimens 81 and 82, which were in the back of the furnace, had more of the deeper pits. Specimens 95 and 96, from the front of the furnace, had very few pits, and none of the deeper ones. However, more data will be needed to draw any firm conclusions about the effect of specimen location in the furnace.

The appearance of typical pits is shown in Figure 2, which depicts portions of the surface of two of the specimens.

TABLE 2. COMPOSITION OF PNL 76-68 GLASS

Oxide	Average Analysis of 3 Bars (%)	Standard Deviation (%)
Al_2O_3	0.84	0.0?
B_2O_3	8.65	0.06
BaO	0.62	0.01
CaO	2.29	0.04
CdO	0.05	0.01
Cr_2O_3	0.50	0.02
Cs_2O	1.21	0.08
Dy_2O_3	0.01	0.00
Eu_2O_3	0.01	0.00
Fe_2O_3	9.08	0.12
Gd_2O_3	0.03	0.01
K_2O	0.09	0.03
La_2O_3	4.89	0.06
MgO	0.18	0.01
MnO_2	0.06	0.00
MoO_3	2.17	0.01
Na_2O	11.60	0.95
Nd_2O_3	1.65	0.01
NiO	0.25	0.03
P_2O_5	0.56	0.08
SiO_2	40.33	0.81
SrO	0.49	0.01
TiO_2	2.86	0.04
ZnO	4.75	0.08
ZrO_2	2.33	0.04
Total	95.50	

TABLE 3. DISTRIBUTION OF PITS ALONG A LINE ACROSS THE SPECIMEN SURFACE (400 HOURS AT 900 C)

Specimen No.	Number of pits of depth indicated					
	< 20μm	20-40μm	40-60μm	60-80μm	80-100μm	100-120μm
81-Side 1	55	4	5	4	6	0
Side 2	48	3	7	5	6	2
82-Side 1	56	10	6	2	5	0
Side 2	33	6	2	0	8	0
91-Side 1	85	9	8	1	0	0
Side 2	68	24	3	1	1	0
92-Side 1	121	4	1	0	0	0
Side 2	50	2	6	0	0	0
95-Side 1	5	5	0	0	0	0
Side 2	6	0	0	0	0	0
96-Side 1	4	0	0	0	0	0
Side 2	4	1	1	0	0	0

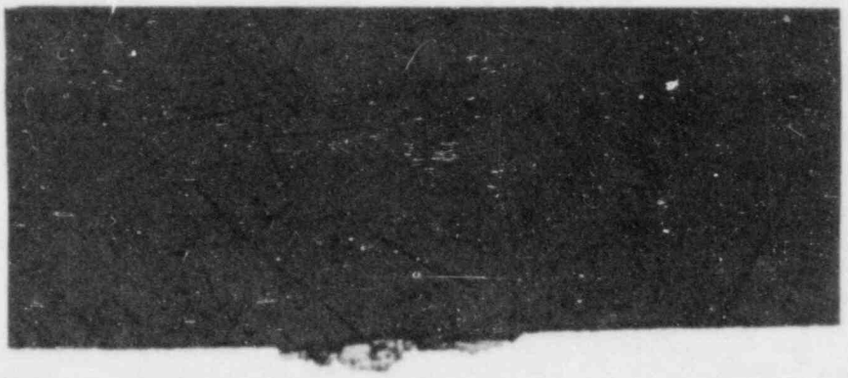

Specimen 96

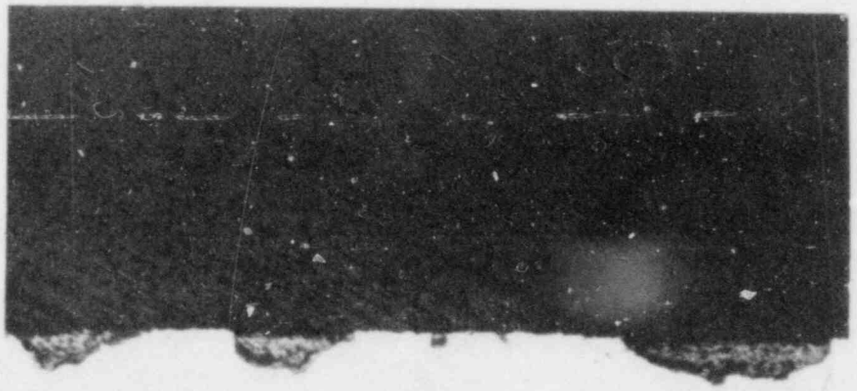

Specimen 82

FIGURE 2. PITS DEVELOPED ON 304L STAINLESS STEEL AFTER 400 HOURS AT 900 C (65X)

3.1.3 Future Work

More data will be obtained regarding the distribution of pits across the surface of the specimens as they are removed from exposure.

The exposures will be continued at 900, 500, and 300 C. The schedule for removal of specimens, based on the assumption of an Arrhenius relationship for temperature effects, is as follows:

900 C	500 C	300 C
400 hrs.	621 hrs.	974 hrs.
750	1165	1826
1330	2065	3239
1930	2997	4700

This schedule is subject to change if the rate of pitting at the lower temperatures indicates that the relationship does not hold.

Selected specimens will be studied under the scanning electron microscope to determine the nature of the corrosion products that develop at the glass-metal interface and to identify the corrosive components.

3.2 External Corrosion

As noted earlier in the report, the DOE had initially favored the use of an outer titanium alloy shell over the structural steel overpack. This resulted in the evaluation of Titanium Grade 12 in slow strain rate and autoclave tests. Of particular concern in the autoclave tests was the effect of heat transfer on corrosion in brine, which was not previously investigated. Analysis of the autoclave test under heat transfer conditions is described in detail below. Also described is the initial effort in the basalt-steel system.

3.2.1 Titanium Grade 12 - Salt System

Analysis of the solution from the second autoclave exposure was completed. This exposure was carried out on Titanium Grade 12 in deaerated Brine A at 250 C under stagnant conditions. Results, given in Table 4, indicated the presence of significant quantities of nickel, chromium, and iron. As discussed in the Annual Report, this contamination apparently occurred as the result of the unexpected generation of HCl in the vapor phase in the autoclave because of hydrolysis of $MgCl_2$ on the heated surfaces. The presence of nickel corrosion products is especially significant since nickel is an inhibitor of localized corrosion of titanium.

Analysis of the electrochemical data from the second autoclave exposure also was completed. Two types of electrochemical measurements were performed: galvanic current and polarization resistance. The objective of the galvanic current experiment was to evaluate the possible

influence of variation in the overpack skin temperature, as a function of location, on corrosion rates; this phenomenon is sometimes referred to as thermogalvanic corrosion. The galvanic current between a heated and an unheated specimen, having equal surface areas, was measured periodically by means of a zero resistance ammeter. The heated specimen was maintained at 270 C by means of an internal resistance heater and thermocouple and appropriate temperature controlling equipment; the unheated specimen was equilibrated at the autoclave temperature (250 C). Prior to performing each measurement, the polarity of the electrodes also was measured. Additional details of the experimental procedure are given in the first Annual Report.

TABLE 4. RESULTS OF INDUCTIVELY COUPLED ARGON PLASMA ANALYSES OF TEST SOLUTION FROM SECOND AUTOCLAVE EXPOSURE OF TITANIUM GRADE 12 IN BRINE A

Only elements having a concentration greater than 1 ppm are reported.

	µg/ml (ppm)
Arsenic	4.7
Boron	210
Calcium	560
Cobalt	590
Chromium	2,600
Copper	310
Iron	3,600
Magnesium	22,000
Manganese	210
Molybdenum	<8
Nickel	9,100
Phosphorus	8.3
Palladium	3.9
Selenium	2.5
Sodium	37,000
Strontium	13
Zinc	7.6

It was found that the heated specimen was noble (positive) to the unheated by about 90 mV throughout the exposure, and that the galvanic current flow was in the direction of the unheated specimen; i.e., the unheated specimen was undergoing galvanic corrosion when in electrical contact with the heated specimen, assuming that the current measured was a corrosion current. Actual current density measurements are given in Figure 3. These data show that the current density fluctuated over the initial 400 hours' exposure in the vicinity of 8×10^{-5} A/cm^2. Converting this current density to a corrosion rate by means of Faraday's Law, and assuming an ionic valence state of +4 for titanium, gives a value of 6.4×10^2 µm/year. This value is more than two orders of magnitude greater than the corrosion rate of the unheated specimen as measured gravimetrically (1.72 µm/year). As discussed in the first Annual Report, a similar discrepancy was observed between corrosion rates of Titanium Grade 12 in Brine A predicted by polarization resistance and those predicted gravimetrically. This discrepancy was attributed to the presence of parasitic redox reactions in the solution which contributed a net current.

It is interesting to note that the corrosion rate of the unheated thermogalvanic specimen measured gravimetrically was greater, by an order of magnitude, than the corrosion rate of the gravimetric specimen from the previous autoclave exposure, or than the corrosion rate of immersed U-bend specimens in the second autoclave exposure. It appears that the galvanic current measurement successfully predicted the direction of the galvanic effect, but not its magnitude. It must be cautioned, however, that in this autoclave exposure, deposit buildup occurred on the heated specimens in the vapor phase, which apparently led to hydrolysis of salts present in the deposits and generation of HCl. The HCl present in the vapor may have accelerated the corrosion rate of the electrodes, which pass through the vapor phase, more than that observed with the immersed U-bend specimens.

During the second autoclave exposure, pressure buildup in the autoclave promoted a leak after approximately 450 hours of exposure. As shown in Figure 3, galvanic currents measured after restart of the autoclave were considerably lower than those measured prior to shutdown. The data taken after autoclave startup, however, are not considered to be reliable since deposit buildup may have impinged on the autoclave head by this time and affected the measurements.

Results of the polarization resistance measurements performed in the second autoclave exposure are summarized in Figure 4. These data show that the polarization resistance values for the heated specimens are higher (1/PR values are lower) than those for the unheated specimens. This suggests that corrosion rates for the heated specimens were lower than those for the unheated specimens which is qualitatively consistent with the results of the galvanic current measurements. Serious problems exist with the data, however. First of all, corrosion rates predicted from the polarization resistance measurements are several orders of magnitude higher than those predicted gravimetrically, as was observed for the unheated specimens in the first autoclave exposure. In

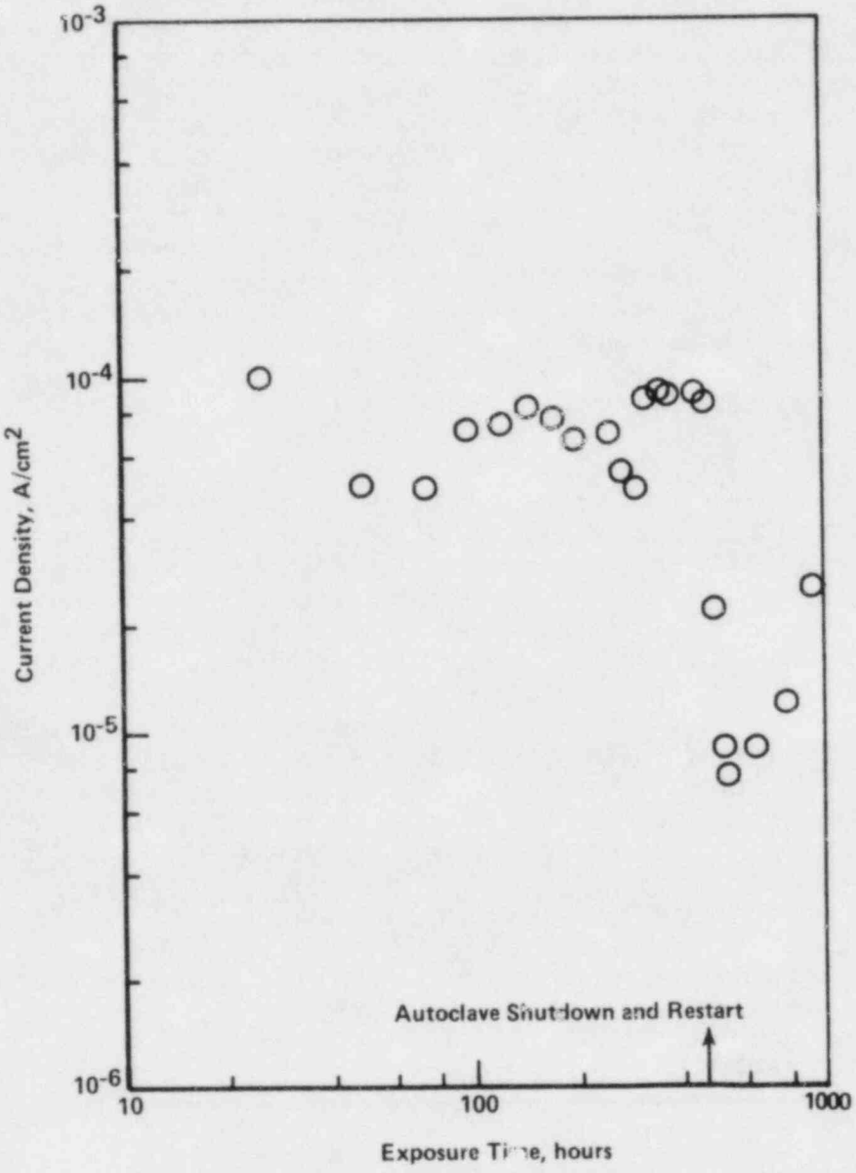

FIGURE 3. GALVANIC CURRENT DENSITY AS A FUNCTION OF EXPOSURE TIME FOR A HEATED TITANIUM GRADE 12 SPECIMEN COUPLED TO AN UNHEATED SPECIMEN (ΔT = 20 C) HAVING EQUAL SURFACE AREAS IN DEAERATED BRINE A AT 250 C

Heated specimens were noble (positive) to unheated specimens throughout exposure

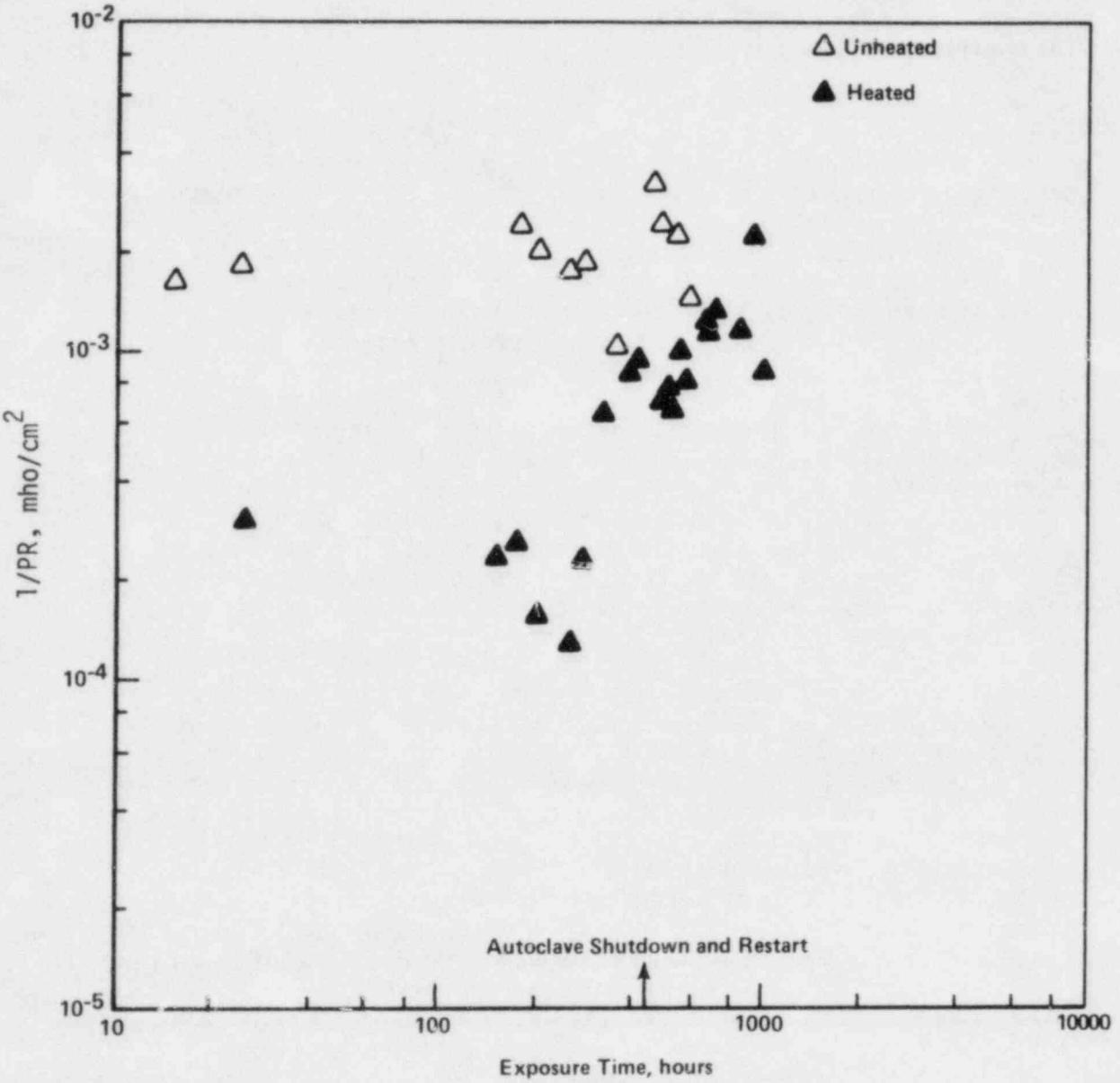

FIGURE 4. 1/PR AS A FUNCTION OF EXPOSURE TIME FOR HEATED (ΔT=20 C) AND UNHEATED TITANIUM GRADE 12 SPECIMENS EXPOSED IN DEAERATED BRINE A AT 250 C

addition, the polarization resistance values for the unheated specimens measured in the second autoclave exposure do not agree well with those reported in the first autoclave exposure. This effect may be the result of the increased concentration of metal ions in the solution, as shown in Table 4. Finally, the measured polarization resistance values for the heated specimens decreased with exposure time after about 300 hours. This may have been a real effect but more probably was a result of impingement of vapor phase deposits onto the autoclave head.

In other work, the final autoclave exposure currently planned for the Titanium Grade 12 - salt system was started up. This exposure is a repeat of the previous exposure in which the effect of heat transfer on corrosion performance was evaluated, with one important exception: a sealed internal canister of Titanium Grade 12 was fitted inside the HASTELLOY Alloy C276 autoclave such that the test environment was isolated from the autoclave head and body. This precaution was taken to prevent contamination of the test solution by corrosion products from the autoclave head, as occurred in the previous autoclave exposure.

In support of the autoclave study, the effect of heat transfer on deposit formation is being studied at ambient pressure. The effect of temperature difference, ΔT, between the heated specimen and the bulk solution on the rate of deposit buildup is being studied at ambient pressure. Although the studies are being performed with the Titanium Grade 12 - salt system, the phenomenon being studied may be relevant to a basalt system where the groundwater has concentrated as a result of evaporation. Thus, a similar experimental technique is planned to study the latter system.

Preliminary results indicate that deposits will readily form on the specimen with a ΔT of 7 C and a bulk solution temperature of 65 C. In contrast to the multicolored deposits which formed in the autoclave tests where significant contamination of the system had occurred, deposits formed at ambient pressure were of a uniform white color (see Figure 5). The deposits were found to contain approximately 68 percent chloride, 15 percent potassium, 13 percent magnesium, 4 percent sodium, and a trace of sulfur, as determined by energy dispersive X-ray spectroscopy. X-ray diffraction analyses of the deposits indicated the presence of KOH, NaCl, and two hydrated magnesium chlorides.

3.2.2 Steel-Basalt System

Preparations were completed for the first autoclave exposure of cast and wrought steel in basalt groundwater. In this test, baseline corrosion data will be generated on the general, crevice, pitting, and stress corrosion performance of cast and wrought steel under stagnant, deaerated conditions in basalt groundwater containing basalt rock obtained from the Umtanum flow. An Ag/AgCl reference electrode and platinum electrodes will be included in the autoclave to measure the Eh of the solution and the corrosion potential of the cast steel. Polarization resistance measurements also will be performed on the cast steel during the exposure period. The results of the electrochemical

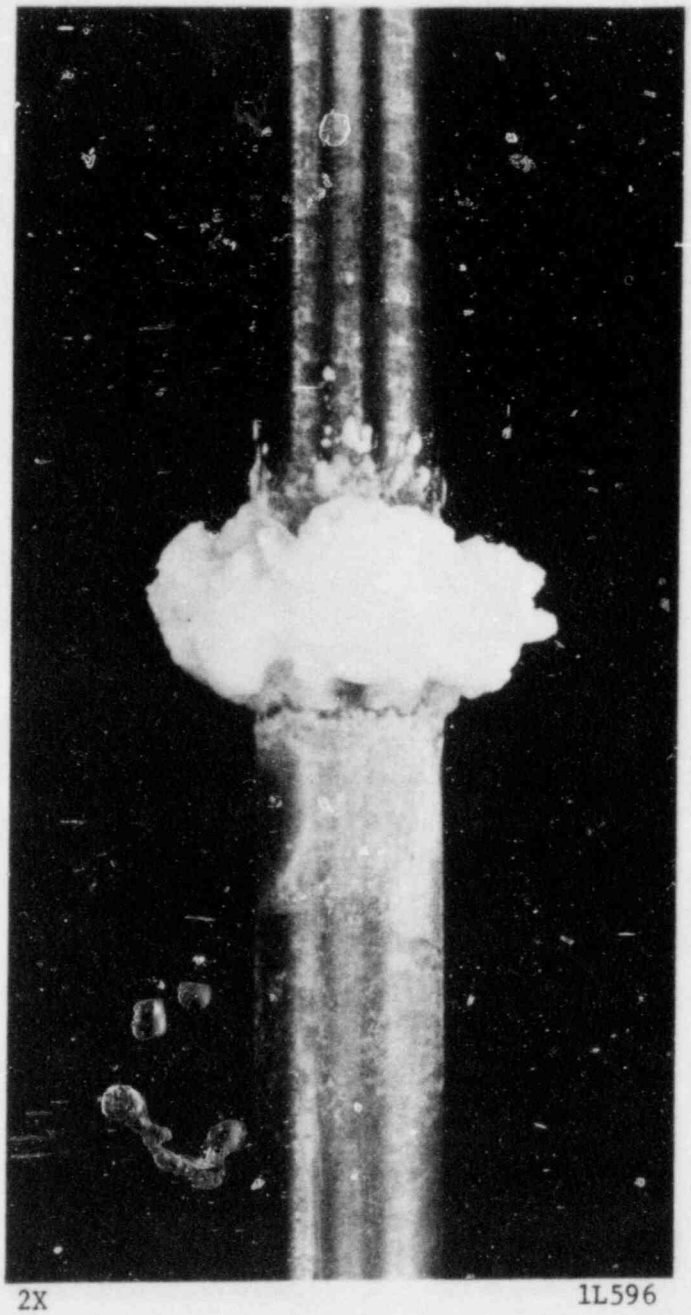

FIGURE 5. DEPOSIT ON TITANIUM GRADE 12 HEAT TRANSFER SPECIMEN EXPOSED FOR 4 HOURS IN NATURALLY AERATED BRINE A AT 65 C WITH A TEMPERATURE DIFFERENCE OF 7 C BETWEEN THE HEATED SPECIMEN AND THE SOLUTION

measurements performed in this system may correlate more closely with actual gravimetric results since the general corrosion rates are expected to be greater and the test solution is less concentrated than in the previous autoclave exposures. Thus, the corrosion currents we are attempting to measure will be larger, and it is less likely that parasitic redox reactions will contribute significant currents.

3.2.3 Future Work

The final autoclave exposure on the Titanium Grade 12 - salt system will be completed and the results will be analyzed. Studies on the influence of heat transfer on deposit buildup on Titanium Grade 12 in Brine A at ambient pressure also will be completed. The first autoclave exposure in the steel-basalt system will be started up. Preparations will be made to start up the second autoclave exposure in the steel-basalt system, in which the effect of solution concentration on corrosion rates will be examined.

3.3 Hydrogen Embrittlement

During the past quarter, tension tests have been conducted in gaseous hydrogen and nitrogen (at 1000 psig and at room temperature in both cases) using specimens made from clean and doped steel castings and from plates that were produced by hot rolling one-half of each of those castings. Two specimen orientations in the castings were identified as being of importance to overpacks: circumferential and axial. Stresses in the circumferential direction (i.e., "hoop" stresses) are likely to arise from (1) residual stresses from solidification, and (2) from the possible buildup of an internal helium pressure in the canister. Axial stresses may occur as a result of bending of the overpack due to mishandling or nonuniform forces from the adjacent rock along the length of the waste package.

Tables 5 and 6 present the tensile data for the cast and wrought specimens, respectively. Quotation marks have been used with the words circumferential and axial because the Battelle castings had square cross sections; the "axial" orientation actually is parallel to the height dimension of the castings whereas the "circumferential" orientation is parallel to width of the castings. Also included in Table 5 are the tensile properties that are to be specified for ASTM A216 Grade WCA steel, a weldable cast steel which is expected to be similar to the alloy that ultimately will be selected by DOE. As shown in Table 5, in the as-cast condition the Battelle steels do not meet the strength requirements of the Grade WCA steel (although they do meet the chemical composition specified). Also, the ductility of the doped steel does not meet the specified level. Tests on some cast specimens that have been fully annealed are planned to determine whether an improvement in ductility can be realized by heat treatment.

TABLE 5. TENSILE PROPERTIES OF CAST STEEL

Test Environment	Ultimate Tensile Strength, ksi	Yield Strength, ksi	Percent Elongation In 1 Inch	Reduction of Area, Percent
	Clean Steel - "Circumferential" Orientation			
Nitrogen	48	19	23	31
Hydrogen	49	18	15	20
	Clean Steel - "Axial" Orientation			
Nitrogen	50	21	29	50
Hydrogen	51	22	28	41
	Doped Steel - "Circumferential" Orientation			
Nitrogen	51	24	26	36
Hydrogen	50	22	15	18
	Doped Steel - "Axial" Orientation			
Nitrogen	51	25	13	16
Hydrogen	50	22	15	20
	ASTM A216 Grade WCA - Unspecified Orientation			
Laboratory Air	60-85	30 Min	24 Min	35 Min

TABLE 6. TENSILE PROPERTIES OF WROUGHT STEEL

Test Environment	Ultimate Tensile Strength, ksi	Yield Strength, ksi	Percent Elongation In 1 Inch	Reduction of Area, Percent
	Clean Steel - Longitudinal Orientation			
Nitrogen	63	42	39	66
Hydrogen	62	42	40	63
	Clean Steel - Transverse Orientation			
Nitrogen	64	41	41	63
Hydrogen	62	39	35	48
	Doped Steel - Longitudinal Orientation			
Nitrogen	67	42	34	53
Hydrogen	67	43	34	40
	Doped Steel - Transverse Orientation			
Nitrogen	65	39	39	63
Hydrogen	65	41	34	37

Figure 6 presents a comparision between the ductility properties (as determined by reduction of area measurement) of the cast and wrought steels in both test orientations. It can be seen that hydrogen reduces the ductility for specimens with a circumferential orientation to a level below that in the Grade WCA specification (35 percent). In addition, the extent of ductility loss is strongly dependent on orientation, with a greater loss in the circumferential orientation. We believe this observation is of particular interest because most acceptance criteria that include tension testing of cast steels do not specify a test orientation. Since the cast steel overpacks reportedly may be produced by centrifugal casting, even greater orientation dependence may be expected because of the greater extent of directional cooling and solidification compared with static castings.

The greater ductility of the doped, as-cast steel tested in hydrogen versus nitrogen (in the axial orientation) actually is a consequence of the inherently low ductility of that steel in nitrogen and the specimen-to-specimen variability of properties in cast steels. Figure 7 shows a representative portion of the fracture surface of a doped, as-cast axially oriented specimen tested in nitrogen, showing a high concentration of manganese sulfide inclusions at the fracture surface. Finally, it should be noted that a straightforward correlation between the hydrogen-embrittlement tendency of cast and wrought steels of identical chemical composition is not presently available, although the correlation may become more apparent when the fracture-toughness testing is conducted.

3.4 Corrosion Correlations

3.4.1 General Corrosion

Initial formulation of a comprehensive physical description of general corrosion of container materials, in the presence of groundwater, was brought near completion during this reporting period. This effort, which is being carried out in conjunction with Professor Digby D. Macdonald of The Ohio State University, has consisted of the development of a mathematical formalism with which to describe the various processes that contribute to general corrosion. With this description, general corrosion is assumed to occur as a result of chemical reaction of the container with the water and the various oxidizing agents contained therein. The latter include hydrogen ions, dissolved oxygen, and various radiolysis products generated by interaction of the gamma field with the water.

Details of the complex electromechanical mass-transport problem associated with general corrosion have been established in mathematical form. In addition, existing experimental data pertinent to the problem have been collected. The description will be set forth in detail, in the near future, in a journal article that is currently in preparation.

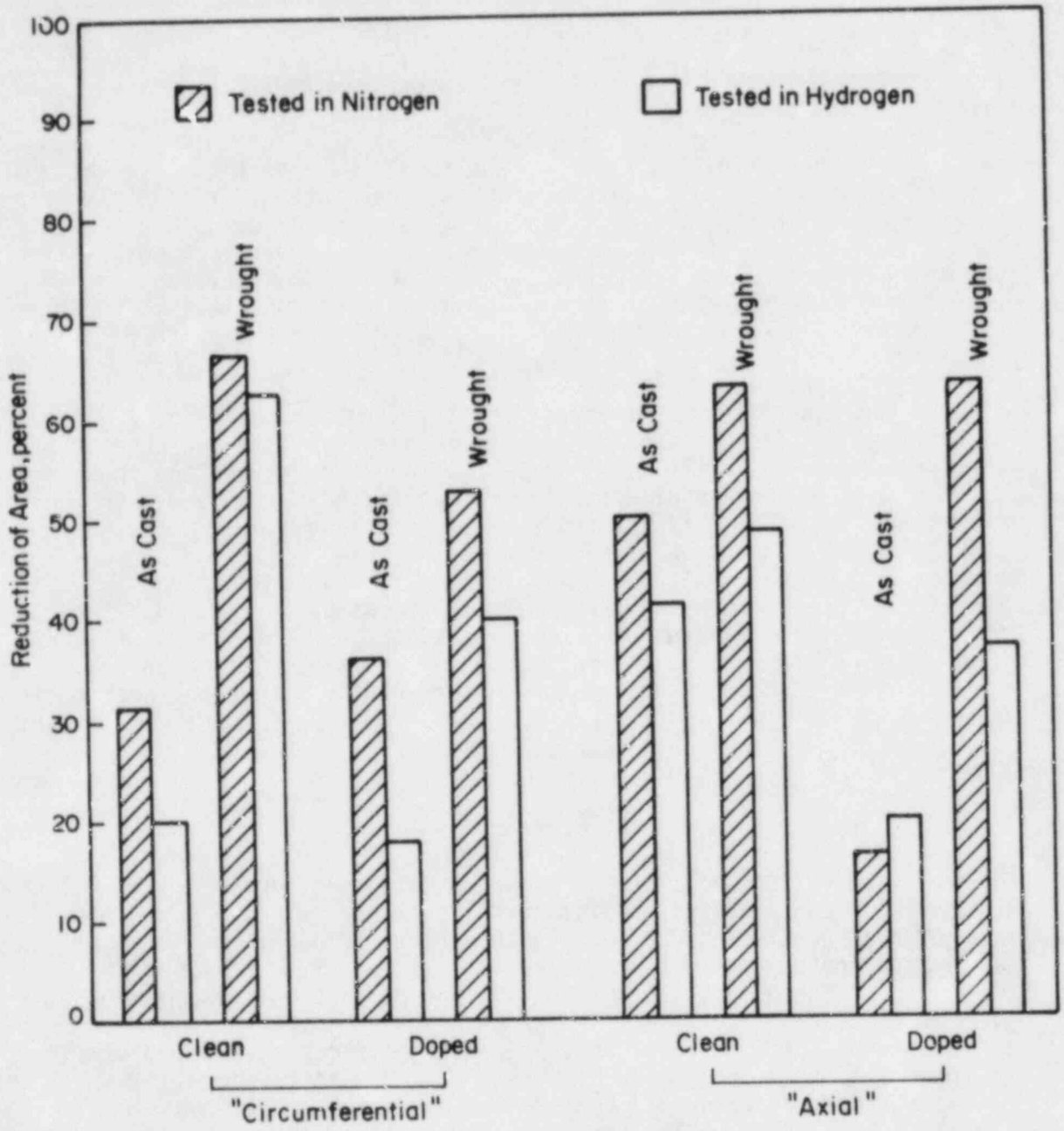

FIGURE 6. DUCTILITY OF BATTELLE STEELS

500X 40422

FIGURE 7. SCANNING ELECTRON MICROGRAPH OF FRACTURE SURFACE OF DOPED, AS-CAST STEEL TESTED IN NITROGEN IN THE "AXIAL" ORIENTATION

The inclusions on the fracture surface all are manganese sulfide

The next stage of development will consist of refinement of the description to a more condensed form that will be based upon the extent to which pertinent data exist as well as the computational complexity associated with numerical solution of the associated system of partial differential equations. Close interaction between the experimenters and the system modelers will be maintained throughout this important aspect of this task.

3.4.2 Pitting Corrosion

In the first Annual Report for this program, a first-cut description of pitting corrosion was presented. The fundamental assumption in that model was that the depth, x, of any given pit varies according to a simple linear relation, i.e., $x = a\,(t-t_o)$ where a is a time-independent parameter characteristic of the process(es) controlling pit growth and t_o is the time at which the pit began to grow. Using this relationship, together with the assumption that the rate at which new pits are generated is some arbitrary function of time, G(t), an expression was derived for the time-dependent frequency distribution for pit depth.

During the past reporting period, this description was extended to account for a more general growth-rate expression, i.e.,

$$x = a\,(t - t_o)^b \tag{11}$$

where $b > 0$. A relationship of this general type actually was used many years ago[1] to describe the variation with time of the maximum pit depth for ferrous specimens in a soil environment. It was pointed out, somewhat more recently[2], that the special case for which $b = 1/3$ has been found to apply to a number of situations, including the maximum pit depth in laboratory tests in almost 200 fresh waters, a 2000-foot industrial water-carrying pipeline for an interval of more than 13 years, and the pitting of aluminum in seawater. A time dependence for pit growth similar to that in Equation 11 has also been discussed by Sato and coworkers[3].

Equation 11 can be used to derive a general expression for the pit-depth frequency distribution, f(x,t), in terms of the parameters a and b and the pit-generation rate, G(t). One can, for example, use either of the two methods discussed in Battelle's first Annual Report to achieve this aim. The final result can thereby be shown to be

$$f(x,t) = \frac{1}{ab}\left(\frac{x}{a}\right)^{\frac{1-b}{b}} G\left(t-\left(\frac{x}{a}\right)^{\frac{1}{b}}\right) \tag{12}$$

for $x < at^b$ and

$$f(x,t) = 0$$

for $x > at^b$.

It was assumed, in the analysis leading to Equation 12, that the parameters a and b are independent of time. However, under actual repository conditions, both are likely to vary with time as the temperature and other conditions vary.

An example of the application of Equation 12 is presented in Figure 8 for the special case b = 0.5. Here, the pit-generation rate is given by

$$G(t) = G_o \{1 - \exp [- (\lambda t)^n]\} \qquad (13)$$

for $t \geq 0$, where G_o and λ are constants, and $G(t) = 0$ for $t < 0$. For this particular form for G(t), the pit-generation rate is zero prior to time t = 0, after which it rises and gradually approaches the constant value G_o. Values of f(x,t) are shown in the figure for several times after the beginning of pit generation. Two important features relative to the change of f(x,t) with increasing time are (1) the fact that the maximum pit depth increases with increasing time (which follows from Equation 11), which would ultimately lead to container penetration, and (2) the fact that the total number of pits, which is proportional to the "area" beneath the distribution function, is clearly increasing with time, as expected from the functional form for G(t).

Continued efforts on the pitting correlation will be directed toward development of a more physically based model, in which pit growth is described in terms of the actual electrochemical processes that contribute to localized corrosion phenomena.

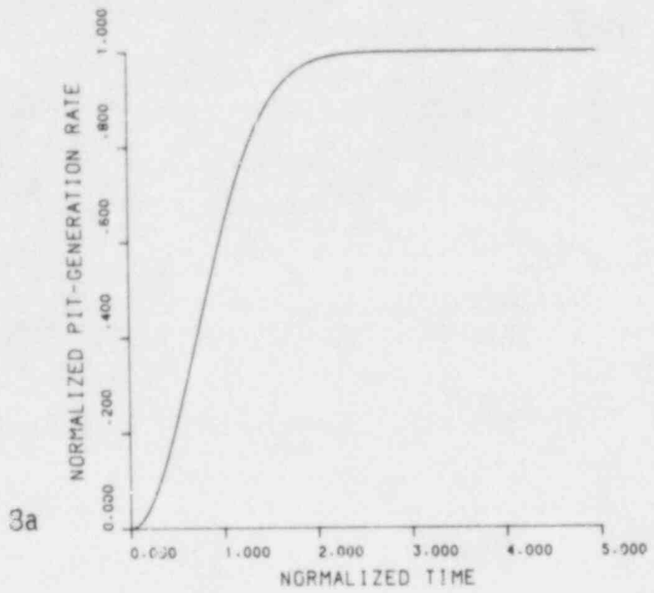

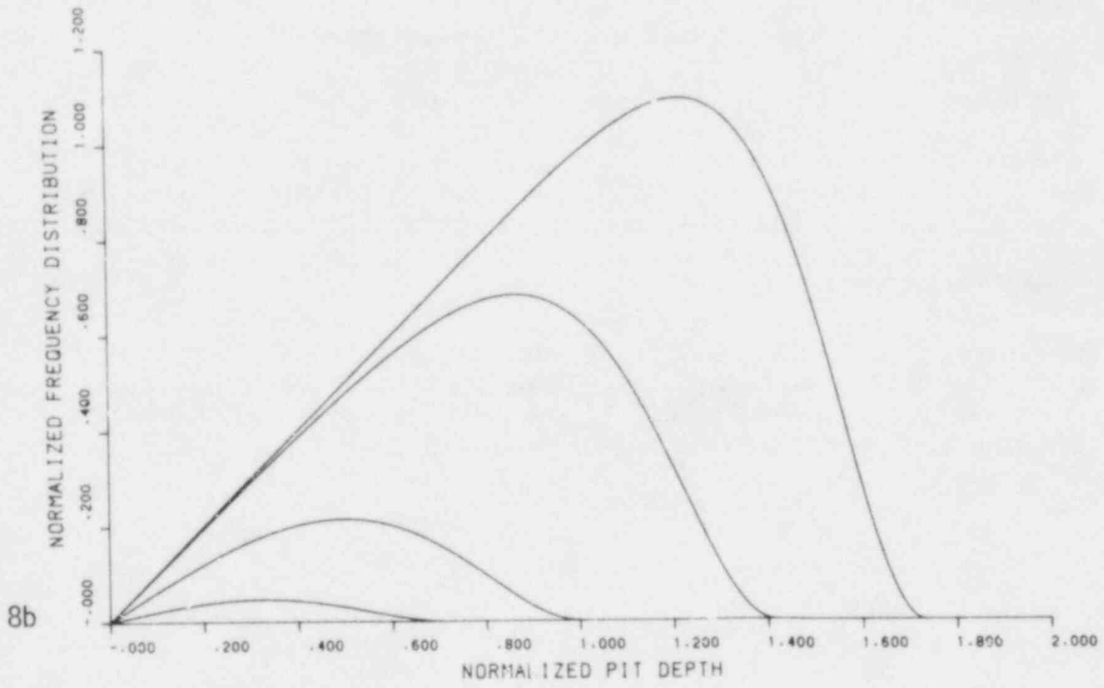

FIGURE 8. VARIATION OF PIT-DEPTH DISTRIBUTION WITH TIME, SHOWN IN 8b (AFTER EQUATION12), FOR THE PIT-GENERATION RATE SHOWN IN 8a (AFTER EQUATION 13) TAKING b = 0.5

The abscissa and ordinate in 8a are λt and $G(t)/G_o$, respectively; the corresponding quantities in 8b are $\lambda^b x/a$ and $ab\lambda^{1-b}\, f(x,t)/G_o$, respectively.

4.0 Integrated System Description

The purpose of this analytical effort is to improve understanding of the long-term behavior of nuclear waste packages placed in deep mined repositories. This understanding is required for evaluation of the waste packages and during licensing of a high level waste repository system. More specifically, the system description will provide the NRC with a means to evaluate the synergisms of the various phenomena which can lead to the degradation of nuclear waste packages and the transport of radionuclides. The system description will thus allow one to study the long-term performance of a waste package in light of the coupled effects of several degradation processes or phenomena. The system study interfaces with an experimental program to provide a means for testing degradation mechanisms with respect to predicting short term experimental results as well as evaluating their long term implications when coupled to other phenomena for long time periods. The system description effort also identifies where data are needed to support licensing decisions regarding the waste package component of the waste isolation system. The waste package is a key element since it is the source of heat and radionuclides which are important factors in the long term assessment of nuclear waste repositories.

Progress this quarter includes improvements to the existing description of fluid flow through a nuclear waste package and development of a comprehensive method for following the transport and decay of all or any radioisotopes of interest. The ability to follow the release of all radioisotopes allows the user to test a system for compliance with the draft EPA standard. The option to follow the behavior of only specific radioisotopes provides a more cost effective means for performing some performance assessment studies.

The method for describing fluid transport used in the system analysis is based on fluid flow through concentric control volumes with well-mixed fluids. The control volumes are defined by the metallic barriers of the waste package. When a metallic barrier separating two control volumes is breached, fluid flow between those control volumes is permitted. In the first version of the system analysis described in the first Annual Report, radionuclide-bearing fluid could only flow from the innermost to the outermost control volume, as shown in Figure 9. This method has been modified so that the fluid in any control volume may be exchanged with the fluid in each adjacent control volume, as illustrated in Figure 10. As in the first version, the fluid in each control volume is assumed to be well mixed. Also, since the fluid is incompressible, the rate of fluid flow into any given control volume is the same as the rate of fluid flow out of that control volume. Furthermore, since the control volumes are concentric, the rate of fluid flow into an adjacent control volume is identical to the return flow rate from that volume. The relative magnitude of the rate of fluid flow between control volumes is determined by the fraction of the surface separating the control volumes which is open to fluid flow. Since the actual geometry[4] is somewhat more complex than concentric cylinders, and since flow patterns

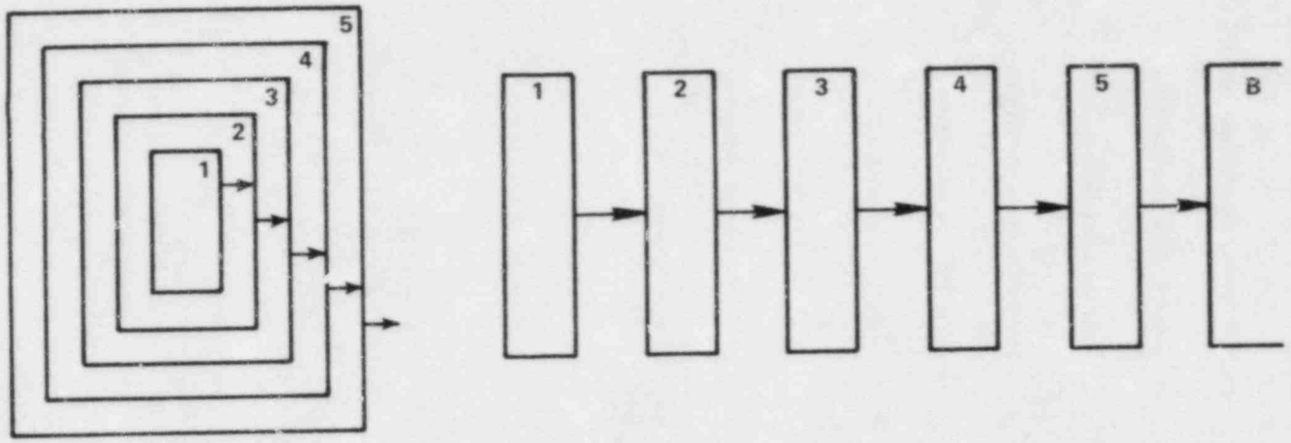

FIGURE 9. METHOD FOR DESCRIBING FLUID FLOW IN FIRST VERSION OF THE SYSTEM ANALYSIS

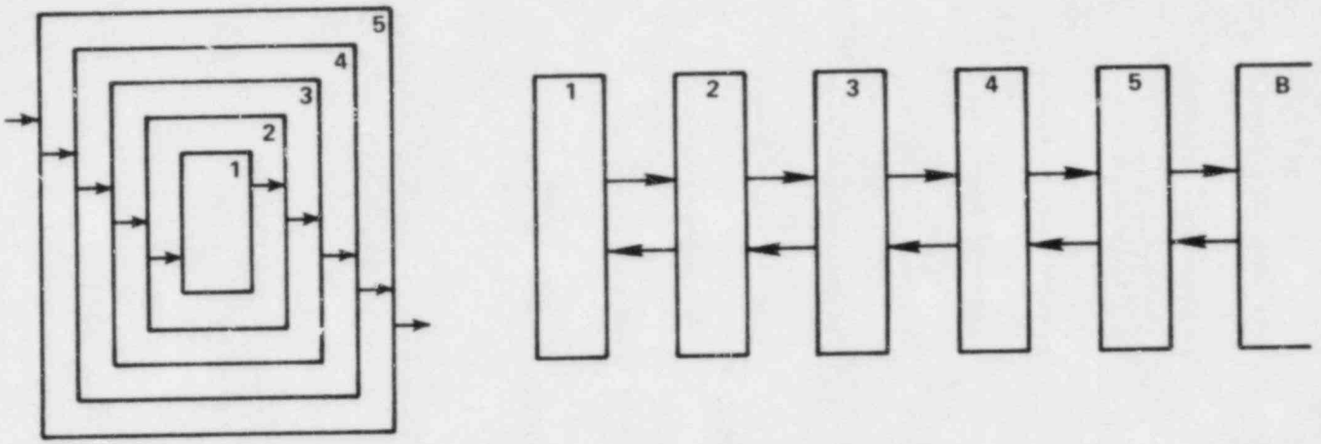

FIGURE 10. MODIFIED METHOD FOR DESCRIBING FLUID FLOW

may be complex, the maximum allowable flow rate between control volumes must be specified by the analyst as some fraction of the fluid flow rate entering the next outermost control volume. In this modified transport analysis, all fluid must enter and leave the waste package through the outermost control volume.

In the differential equations describing transport through the waste package, the rate of transfer of the inventory of an element from the n to the (n+1) control volume is given by:

$$\frac{F(n,n+1)\ N(n)}{V(n)}$$

where N(n) is the number of moles of an element present in control volume n and V(n) is the volume. The rate of transfer of material from control volume (n+1) to control volume n is given by:

$$\frac{F(n+1,n)\ N(n+1)}{V(n)}$$

where the flow rates linking two control volumes are equal [i.e., $F(n+1,n) = F(n,n+1)$]. The fluid flow source rates for a control volume which is neither the innermost nor the outermost has, therefore, two source rates and two sink rates. The source rates are from fluid flowing in from the two adjacent control volumes [i.e., $F(n-1,n)$ $F(n+1,n)$]. The mass flow rates to the control volume n from these control volumes is represented in the transport equations as:

$$\frac{F(n-1,n)\ N(n-1)}{V(n-1)}$$

and

$$\frac{F(n+1,n)\ N(N+1)}{V(n+1)}$$

The two fluid flow sink rates for this control volume are given by the rate of fluid flow to the adjacent control volumes [(i.e., $F(n,n-1)$ and $F(n,n+1)$]. In the transport equations, these mass flow loss rates for a control volume n are given by:

$$\frac{F(n,n-1)\ N(n)}{V(n)}$$

and

$$\frac{F(n,n+1)\ N(n)}{V(n)} \quad .$$

The innermost control volume (with n=1), as can be seen in Figure 9, can only exchange fluid with the next innermost control volume (with n=2). The innermost control volume therefore has only one fluid flow source and sink rate namely F(1,2) and F(2,1) and these flow rates are equal. The outermost control volume, as can be seen in Figure 10, exchanges fluid with both the backfill region and the next innermost control volume.

The radioactive decay and transport of the fission product isotopes will be handled in a manner similar to the current treatment of the actinide isotopes in the first system description. This will allow the analyst to evaluate the performance of a waste package with respect to all isotopes or just a select few if desired. In this treatment, the radioactive decay and buildup of each isotope will be calculated with a modified version of ORIGEN-79.[5] The transport of radioisotopes will be calculated with respect to elemental inventories.

In the near future, attention will be focused on developing methods for precipitation and dissolution analysis.

5. SUPPORT ACTIVITIES

There are three major supporting technical activities which provide input to all three generic tasks. These are water chemistry studies, accelerated test planning/statistics, and quality assurance. The major accomplishments during this reporting quarter are given below.

5.1 Water-Chemistry Studies

Effects of water chemistry pertain to all the various degradation processes that result from the presence of groundwater, including waste-form dissolution as well as general and localized corrosion of container materials. For this reason, a method for water-chemistry analysis is being developed that will play an integral role in describing the overall waste package. Recently obtained results in this area are now described.

Notable activities in water chemistry during the current quarter fell primarily into two categories: testing of the water-chemistry analysis that has been incorporated into the system description and calculations of the effects of groundwater concentration.

One potential shortcoming of the water-chemistry analysis, in its current form, is the limited number of species that are included. As a test, we have compared calculations and experimental results for natural and synthetic groundwaters. As part of the Basalt Waste Isolation Project, chemical analyses have been carried out on Grande Ronde basalt groundwater. According to Jones,[6] this groundwater "would be the most likely to migrate into either of the two candidate repository horizons within the Grande Ronde Basalt (i.e., the Umtanum and Middle Sentinel Bluffs flows)." For experimental convenience, Rockwell Hanford developed a synthetic groundwater which closely reproduces the actual groundwater. The compositions of these two solutions are given in Table 7. Additional species are present in the natural groundwater in very small concentrations.

As a measure of the accuracy of the water-chemistry analysis, we have selected the value of the calculated pH. At a given temperature, pH is the most important single variable in the determination of the solubility and rate of dissolution of a silicate glass. Accordingly, the accuracy of the predictions of any system model are heavily dependent on the accuracy with which pH may be calculated.

Three values for the pH of the synthetic groundwater have been obtained, two theoretical and one experimental. All of these values are for a temperature of 25°C. The first theoretical value was determined in the water-chemistry analysis that has been included in the system description. Because of the small number of species included, it was necessary to lump sodium and potassium as sodium, and chlorine and fluorine as chlorine. This method, which handles 16 solute species, yielded a calculated pH of 9.90. The second theoretical value was calculated using the program WATEQ of Truesdell and Jones.[7] This program considers

109 solute species, and it was not necessary to lump any of the measured concentrations. However, WATEQ does not normally require that the electroneutrality condition be satisfied, so it was necessary to run the program repeatedly until a pH was found which made the solution electrically neutral. This pH is 9.88. By comparison, the experimental value of the pH of the synthetic groundwater as reported by Jones is 9.74 ± 0.10.

Some of the assumptions that were made in analyzing the water chemistry seem to be severe; many solute species were ignored, and the alkali metals were lumped together, as were the halogens. However, these assumptions may in fact be less important than they appear, since the neglected species generally have very low concentrations, and since the alkali metals are chemically similar, as are the halogens.

TABLE 7. COMPOSITION OF ACTUAL AND SYNTHETIC GRANDE RONDE GROUNDWATER, 25 C

Constituent	Molarity	
	Actual	Synthetic
Na	15.8×10^{-3}	15.6×10^{-3}
K	87.8×10^{-6}	87.8×10^{-6}
Ca	69.0×10^{-6}	69.0×10^{-6}
Mg	1.315×10^{-6}	1.315×10^{-6}
F	1.76×10^{-3}	1.76×10^{-3}
Cl	8.75×10^{-3}	8.81×10^{-3}
SO_4	1.802×10^{-3}	1.805×10^{-3}
C*	1.267×10^{-3}	0.896×10^{-3}
SO_2	1.267×10^{-3}	1.268×10^{-3}

*Total inorganic carbon.

Typographical errors appearing in Table 1 of Reference 6 have been corrected here.

With regard to glass dissolution in basalt groundwaters, it is clear that there is little to be gained by including additional species. Increasing the number of solute species from 16 to 109 reduced the error in pH insignificantly, from 0.16 to 0.14. It should be noted, too, that Jones's procedure for preparing synthetic groundwater includes the addition of NaOH or HCl solutions to achieve the correct pH.

Both our current methods for water-chemistry analysis and the WATEQ code yield acceptable values for the pH of synthetic basalt groundwater. On this basis, it is reasonable to conclude that the current water-chemistry analysis is sufficiently detailed for use in describing the chemistry of a basalt groundwater. Additional species may still be necessary, however, to describe more concentrated groundwaters or the effects of the repository on the groundwater composition.

During the operational period of the repository, it is expected that self-heating of the waste packages will cause significant evaporation of water in the surrounding rock. After closure, hydrostatic pressure will rise and, eventually, temperature will fall, so that the groundwater will come in contact with the waste package. However, the composition of the groundwater near the waste package may be changed due to the previous evaporation.

In progress are calculations regarding the composition of concentrated groundwater. These calculations use the composition of the Grande Ronde basalt water as reported by Jones[6] plus 9 ppb of iron and 10 ppb of aluminum. WATEQ is being used so that all elements may be treated correctly.

Determination of a concentrated groundwater composition is not straightforward because the kinetics of the various processes are not well known. If it is assumed that the precipitation processes are very slow, the composition of the concentrated groundwater can be found by simply scaling up the concentrations of all the dissolved elements. If, on the other hand, it is assumed that the precipitation processes are very fast, the composition can be found from solubility calculations. Under repository conditions, neither of these idealizations is likely to hold for all processes. Additional work is necessary in this area.

5.2 Accelerated Test Planning/Statistics

A baseline experiment for the nonaqueous internal corrosion experimental program was developed jointly with the statistician and the experimenter. This experiment will study corrosion phenomena associated with the interaction of glass and stainless steel at various accelerated temperature conditions.

The responses to be measured are the extent of general corrosion, the extent of pitting corrosion, and the chemical species present in pitted areas. The primary experimental variables are exposure temperature and time. For each temperature, the extent of corrosion is studied at multiple times. The maximum test temperature is 900 C. Based on data

reported in the literature, a tentative average trend curve of general corrosion versus time has been derived for planning purposes. Tentative exposure times at 900 C have been established based on this curve. These times will be modified during the course of the experiment if the observed corrosion rates are found to differ substantially from the rates assumed for planning purposes.

As a planning assumption, an Arrhenius relation has been used to reflect temperature dependence of corrosion levels. Tentative exposure times at the lower temperatures have been based on predictions from the Arrhenius relation. These times will be modified during of the experiment if the observed corrosion rates are found to differ substantially from the rates assumed for planning purposes.

The details of the experiment layout, measurement procedures, and data analysis considerations will be described in detail in the next quarterly report.

The search is continuing for statistical reference literature dealing with corrosion data, models, and statistical analyses that describe the time trends of general and pitting corrosion as functions of stress factors (such as temperature and chemical constituents) and that illustrate fitting such models to the data. Thus far, no such statistical literature specific to the corrosion area has been found although discussions of analogous problems in other areas (e.g., crack growth, dielectric breakdown strength) have been located.

During the coming quarter, interaction will continue with the modelers and experimenters to analyze data generated in the leaching and internal corrosion experimental programs and to help plan further experimental efforts. Statistical methodology questions associated with the design and analysis of accelerated tests will be explored to describe various types of corrosion phenomena.

5.3 Quality Assurance

During the report period, seventeen quality assurance procedures were prepared, reviewed, and approved by authorized personnel. Two other procedures were revised and approved, while another six were written but have not yet received final approval. A listing of all the procedures which have been approved, as well as those which are in various stages of review, are given in Table 8. In addition, Table 8 also lists several procedures which are to be prepared.

TABLE 8. STATUS OF NRC WASTE PACKAGING PROGRAM QA PROCEDURES

Procedure No.	Title	Status
WF-PP-1 Revision 0	Procedures for Record Keeping and Documentation for NRC Waste Form System Model Development	Approved
WF-PP-5 Revision 0	Procedures for Record Keeping and Documentation for Separate Effects Model Development	Approved
WF-PP-10 Revision 0	Laboratory Procedure for Preparation of Glasses for NRC Waste Form Project	Approved
WF-PP-11 Revision 0	Laboratory Procedures for Preparation of Teflon-Leach Containers	In Review
WF-PP-14 Revision 0	Laboratory Procedure for Leaching Glass Samples	In Review
WF-PP-20 Revision 0	Procedure for Determining the Corrosion Rates of Alloys at High Temperatures	Approved
WF-PP-25 Revision 0	Procedure for Preparation of Carbon-Steel Castings	Approved this quarter
WF-PP-26 Revision 0	Procedure for Preparation of Steel Hydrogen-Embrittlement-Test Specimens	Approved this quarter
WF-PP-27 Revision 1	Procedure for J-Testing Compact Tension Specimens	Revised and approved this quarter
WF-PP-28 Revision 1	Procedure for Performing Tension Tests of Steel Specimens	Revised and approved this quarter

TABLE 8. CONTINUED

Procedure No.	Title	Status
WF-PP-30 Revision 0	Laboratory Procedure for Preparation, Cleaning, and Evaluation of Titanium Grade-12 Specimens for Corrosion Studies of the Overpack Performance for the NRC Waste Packaging Program	Approved this quarter
WF-PP-31 Revision 0	Laboratory Procedure for Preparation, Cleaning, and Evaluation of Cast and Wrought Carbon Steel Specimens for Corrosion Studies of the Overpack Performance for the NRC Waste Packaging Program	Approved tnis quarter
WF-PP-32 Revision 0	Procedure for Preparation of Brine A for Corrosion Testing Under Simulated Repository Conditions	Approved this quarter
WF-PP-33 Revision 0	Procedure for Preparation of Simulated Basalt Groundwater Solution	In Review
WF-PP-33.1 Revision 0	Procedure for Preparation of Basalt Rock for Use in Corrosion Studies for the NRC Waste Packaging Program	Approved this quarter
WF-PP-34 Revision 0	Procedure for Preparation of Simulated Tuff Groundwater Solutions	To be written
WF-PP-35 Revision 1	Procedure for Performing Autoclave Exposures for Corrosion Tests in Simulated Brines	Approved this quarter
WF-PP-35.1 Revision 0	Procedure for Performing Autoclave Exposures for Corrosion Tests in Simulated Brines Using Sealed Internal Canister	Approved this quarter

TABLE 8. CONTINUED

Procedure No.	Title	Status
WF-PP-36 Revision 0	Procedure for Performing Stagnant Autoclave Exposures for Corrosion Tests in Simulated Basalt or Tuff Groundwaters	In review
WF-PP-37 Revision 0	Laboratory Procedure for Preparing Polarization Resistance Specimens, Performing Polarization Resistance Measurements and Evaluating Polarization Resistance Data	Approved this quarter
WF-PP-37.1 Revision 0	Laboratory Procedure for Performing Eh and Corrosion Potential Measurements in Autoclave Exposures in Simulated Basalt and Tuff Groundwater	In review
WF-PP-38 Revision 0	Procedure for Preparing and Evaluation of U-Bend Specimens for Stress Corrosion Studies of Overpack Materials for the NRC Waste Packaging Project	Approved this quarter
WF-PP-38.1 Revision 0	Procedure for Preparing and Evaluating 3 Point Bend Beam Specimens for Stress Corrosion Studies of Overpack Materials for NRC Waste Package Program	In review
WF-PP-39 Revision 0	Procedure for Preparation, Testing and Evaluating Crevice Corrosion Specimens of Titanium Grade-12 and Cast Steel	Approved this quarter
WF-PP-40 Revision 0	Laboratory Procedures for Preparation, Cleaning, and Evaluation of Thermogalvanic and Heat-Transfer Specimens	Approved this quarter
WF-PP-41 Revision 0	Laboratory Procedures for Determination of Corrosion Rates Under Heat-Transfer Conditions	Approved this quarter
WF-PP-42 Revision 0	Laboratory Procedures for Determination of Thermogalvanic Corrosion Rates	Approved this quarter

TABLE 8. CONTINUED

Procedure No.	Title	Status
WF-PP-43 Revision 0	Procedure for Welding Titanium Grade-12 Plate for Use In Corrosion Studies of Overpack Materials for NRC Waste Isolation Project	Approved this quarter
WF-PP-44 Revision 0	Procedure for Welding Cast and Wrought Steel Specimens	To be written
WF-PP-45 Revision 0	Laboratory Procedures for Preparing and Evaluating Slow Strain-Rate Specimens and for Performing Slow Strain-Rate Tests	Approved this quarter
WF-PP-46 Revision 0	Procedures for Preparation of Titanium Grade-12 Corrosion Specimens with Metallic Iron Embedded in the Surface	Approved this quarter

6. REFERENCES

(1) M. Romanoff, Underground Corrosion, National Bureau of Standards Circular 579 (April, 1957), pp. 38, 47, 64, 72.

(2) H. P. Godard, W. B. Jepson, M. R. Bothwell, and R. L. Kane, The Corrosion of Light Metals, John Wiley & Sons, Inc. (New York, 1967), pp. 60, 61.

(3) N. Sato, T. Nakagawa, K. Kudo, and M. Sakashita, "Chloride Pitting Dissolution of Rotating Stainless Steel Electrode in Acid Solution", in Localized Corrosion, R. W. Staehle, B. F. Brown, J. Kruger, and A. Agrawal (Editors), NACE-3, Nat. Assoc. of Corrosion Engineers (Houston, Texas, 1974), p. 447.

(4) "Engineered Waste Package Conceptual Design: Defense High Level Waste (Form 1), and Spent Fuel (Form 2) Disposal in Salt", ONWI-438 (April 1983).

(5) M. J. Bell, "ORIGEN-79: Isotope Generation and Depletion Code - Matrix Exponential Method", Radiation Shielding Information Center, Oak Ridge, TN, CCC-217.

(6) T. E. Jones, "Reference Material Chemistry - Synthetic Groundwater Composition", RHO-Bw-St-37 P, April, 1982.

(7) A. H. Truesdell and B. F. Jones, "WATEQ, A Computer Program for Calculating Chemical Equilibria of Natural Waters", U.S. Geol. Surv. J. Res. 2, 223, 1974.

DISTRIBUTION LIST

Kyo S. Kim (20)
Mail Stop 1130ss
U.S. Nuclear Reg. Commission
Washington, D.C. 20555

Martin Seitz
Argonne National Lab.
Argonne, IL 60439

Martin J. Steindler
Argonne National Lab.
Argonne, IL 60439

Donald G. Schweitzer
Brookhaven National Lab.
Upton, NY 11973

Peter Soo
Brookhaven National Lab.
Upton, NY 11973

David Martin
Iowa State University
Ames, IA 50011

Harold Wollenberg
Lawrence Berkeley Lab.
Berkeley, CA 94720

Nestor Ortiz
Sandia National Lab.
Albuquerque, NM 87185

Pedro B. Macedo
Catholic University of America
Washington, D.C. 20064

Robert Williams
Electric Power Research Institute
P.O. Box 10412
Palo Alto, CA 94301

William P. Reed
U.S. Department of Commerce
National Bureau of Standards
Washington, D.C. 20234

Ray Walton
U.S. Department of Energy
Washington, D.C. 20545

John E. Mendel
Materials Characterization Center
Pacific Northwest Lab.
Richland, WA 99352

John Crandall
Savannah River Lab.
Aiken, SC 29801

Edward J. Hennelly
Savannah River Lab.
Aiken, SC 29801

Samuel J. Basham
Office of Nuclear Waste Isolation
Battelle Memorial Institute
505 King Avenue
Columbus, OH 43201

Michael Smith
Basalt Waste Isolation Projects
Rockwell Hanford Operation
Richland, WA 99352

Kenneth Russell
Department of Materials Science
and Engineering
Massachusetts Institute of
Technology
Cambridge, MA 02139

Robert H. Doremus
Materials Engineering Department
Rensselaer Polytechnic Institute
Troy, NY 12181

David C. Kocher
Oak Ridge National Lab.
P.O. Box X
Oak Ridge, TN 37830

Stanley Wolf
DOE/BES
Washington, D.C. 20585

Neville Moody
Sandia Livermore Lab.
Livermore, CA 94550

Donald E. Clark
ONWI
Battelle Memorial Institute
505 King Avenue
Columbus, OH 43201

Martin A. Molecke
Sandia National Lab.
Albuquerque, NM 87185

Neville Pugh
National Bureau of Standards
Washington, D.C. 20234

Nicholas Grant
Department of Metallurgy
Massachusetts Institute
of Technology
Cambridge, MA 02139

Jerome Kruger
Corrosion Section
National Bureau of Standards
Washington, D.C. 20234

Tae-Moon Ann
Brookhaven National Lab.
Upton, NY 11973

Lynn Hobbs
Department of Materials Science
Massachusetts Institute of Technology
77 Massachusetts Avenue
Cambridge, MA 02139

Richard E. Westerman
Pacific Northwest Lab.
P.O. Box 999
Richland, WA 99352

Thomas D. Chikalla
Pacific Northwest Lab.
P.O. Box 999
Richland, WA 99352

Larry Hench
University of Florida
Gainesville, FL 32611

Davis E. Clark
University of Florida
Gainesville, FL 32611

Joseph Mascara
MS 5650 NL
U.S. Nuclear Reg. Comm.
Washington, DC 20555

NRC FORM 335 (11-81)

U.S. NUCLEAR REGULATORY COMMISSION

BIBLIOGRAPHIC DATA SHEET

1. REPORT NUMBER (Assigned by DDC)
NUREG/CR-3427, Vol. 1

4. TITLE AND SUBTITLE (Add Volume No., if appropriate)
Long-Term Performance of Materials Used for High-Level Waste Packaging
Quarterly Report, April - June 1983

2. (Leave blank)

3. RECIPIENT'S ACCESSION NO.

7. AUTHOR(S)
Compiled by D. Stahl, N.E. Miller

5. DATE REPORT COMPLETED
MONTH: June | YEAR: 1983

9. PERFORMING ORGANIZATION NAME AND MAILING ADDRESS (Include Zip Code)
Battelle Columbus Laboratories
505 King Avenue
Columbus, OH 43201

DATE REPORT ISSUED
MONTH: August | YEAR: 1983

6. (Leave blank)

8. (Leave blank)

12. SPONSORING ORGANIZATION NAME AND MAILING ADDRESS (Include Zip Code)
Division of Health, Siting and Waste Management
Office of Nuclear Regulatory Research
U.S. Nuclear Regulatory Commission
Washington, DC 20555

10. PROJECT/TASK/WORK UNIT NO.

11. FIN NO.
B6764

13. TYPE OF REPORT
Quarterly

PERIOD COVERED (Inclusive dates)
April - June 1983

15. SUPPLEMENTARY NOTES

14. (Leave blank)

16. ABSTRACT (200 words or less)

This quarterly report describes the experimental program for investigating waste form degradation. The mathematical description of waste glass dissolution has been refined. Groundwater corrosion studies have been nearly completed for titanium and are under way for steel container materials. Internal glass-stainless steel corrosion tests have been initiated and pitting chemical interactions are being evaluated. A first-cut physical description of general corrosion of container materials in contact with groundwater is near completion. An improved description of fluid flow through a nuclear waste package was developed, along with a method for tracking radioisotopes. Efforts continue in water-chemistry and accelerated testing.

17. KEY WORDS AND DOCUMENT ANALYSIS

17a. DESCRIPTORS

high level waste
waste package
waste form/container/overpack

17b. IDENTIFIERS/OPEN-ENDED TERMS

18. AVAILABILITY STATEMENT
Unlimited

19. SECURITY CLASS (This report)
Unclassified

21. NO. OF PAGES

20. SECURITY CLASS (This page)
Unclassified

22. PRICE
$